International Journal of Thermophysics, Vol. 25, No. 3, May 2004 (© 2004)

Thermal Behavior of a Multi-layered Thin Slab Carrying Periodic Signals under the Effect of the Dual-Phase-Lag Heat Conduction Model

M. A. Al-Nimr,[1,2] M. Naji,[1] and R. I. Abdallah[1]

Received October 16, 2003

The thermal behavior of a two-layered thin slab carrying periodic signals under the effect of the dual-phase-lag heat conduction model is investigated. Two types of periodic signals are considered, a periodic heating source and a periodic imposed temperature at the boundary. The deviations among the predictions of the classical diffusion model, the wave mode, and the dual-phase-lag model are investigated. Analytical closed-form solutions are obtained for the temperature distribution within the slab. The effect of the angular frequency, thickness of the plate, dimensionless thermal relaxation time, dimensionless phase-lag in temperature gradient, thermal conductivity, and thermal diffusivity on the temperature distribution of the slab was studied. It is found that the deviations among the three models increase as the frequency of the signals increases and as the thickness of the plate decreases. It is found that the use of the dual-phase-lag heat conduction model is necessary when the metal film thickness is of order 10^{-6} m and the angular frequency of the signals is of order $10^{12}\text{rad} \cdot \text{s}^{-1}$.

KEY WORDS: composite slab; dual-phase-lag model; hyperbolic heat conduction model; non-Fourier heat conduction model; periodic heating source.

1. INTRODUCTION

For situations involving very low temperature near absolute zero, a heat source such as a laser or microwave of extremely short duration or with a very high frequency, and very high temperature gradient, heat is found to propagate at a finite speed. To account for the phenomena involving

[1] Department of Mechanical Engineering, Jordan University of Science and Technology, P.O. Box 3030, Irbid 22110, Jordan.
[2] To whom correspondence should be addressed. E-mail: malnimr@just.edu.jo

0195-928X/04/0500-0949/0

the finite propagation speed of the thermal wave, the classical Fourier heat flux model should be modified. Cattaneo [1] and Vernotte [2] suggested independently a modified heat flux model in the form of

$$\mathbf{q}(t+\bar{\tau},\mathbf{r}) = -k\nabla T(t,\mathbf{r}) \tag{1}$$

The constitutive law of Eq. (1) assumes that the heat vector (the effect) and the temperature gradient (the cause) across a material volume occur at different instants of time, and the time delay between the heat flux and the temperature gradient is the relaxation time $\bar{\tau}$. The first-order expansion of q in Eq. (1) with respect to t bridges all the physical quantities at the same time. It results in the expansion,

$$\mathbf{q}(t,\mathbf{r}) + \bar{\tau}\frac{\partial \mathbf{q}}{\partial t}(t,\mathbf{r}) = -k\nabla T(t,\mathbf{r}) \tag{2}$$

In Eq. (2) it is assumed that $\bar{\tau}$ is small enough so that the first-order Taylor expansion of $q(t+\bar{\tau},r)$ is an accurate representation for the conduction heat flux vector. The equation of energy conservation for such a problem is given as

$$\rho c\frac{\partial T}{\partial t} = -\nabla\cdot\mathbf{q} + g \tag{3}$$

Elimination of q between Eqs. (2) and (3) leads to the classical hyperbolic heat conduction equation,

$$\frac{1}{\alpha}\frac{\partial T}{\partial t} + \frac{\bar{\tau}}{\alpha}\frac{\partial^2 T}{\partial t^2} = -\nabla^2 T + \frac{g}{k} + \frac{\bar{\tau}}{k}\frac{\partial g}{\partial t} \tag{4}$$

To remove the temperature gradient driving force (lead) assumption made in the thermal wave model, as proposed in Eq. (1), the-dual phase-lag model is proposed [3–5]. The dual-phase-lag model allows either the temperature gradient (cause) to drive the heat flux vector (effect) or the heat flux vector (cause) to drive the temperature gradient (effect) in the transient process. Mathematically, this can be represented by [3–5]

$$q(t+\bar{\tau}_q,r) = -k\nabla T(t+\bar{\tau}_t,r) \tag{5}$$

For the case of $\bar{\tau}_T > \bar{\tau}_q$, the temperature gradient established across a material volume is a result of the heat flow, implying that the heat flux vector is the cause and the temperature gradient is the effect. For $\bar{\tau}_T < \bar{\tau}_q$, on the other hand, heat flow is induced by the temperature gradient established at an earlier time, implying that the temperature gradient is the

cause, while the heat flux vector is the effect. The first-order approximation of Eq. (5) yields

$$q(t,r)+\bar{\tau}_q\frac{\partial q}{\partial t}(t,r)=-k\left[\Delta T(t,r)+\bar{\tau}_t\frac{\partial}{\partial t}\left[\Delta T(t,r)\right]\right] \tag{6}$$

Elimination of q between Eqs. (3) and (6) leads to the heat conduction equation under the dual-phase-lag effect:

$$\frac{1}{\alpha}\frac{\partial T}{\partial t}(t,r)+\frac{\bar{\tau}_q}{\alpha}\frac{\partial^2 T}{\partial t^2}(t,r)=\nabla^2 T(t,r)+\bar{\tau}_T\frac{\partial}{\partial t}\left[\nabla^2 T(t,r)\right]+\frac{1}{k}\left[g+\bar{\tau}_q\frac{\partial g}{\partial t}(t,r)\right] \tag{7}$$

In the absence of the temperature gradient phase-lag ($\bar{\tau}_T=0$), Eq. (7) reduces to the classical hyperbolic heat conduction as described by Eq. (4), also, in the absence of two phase-lags ($\bar{\tau}_T=\bar{\tau}_q=0$), Eq. (7) reduces to the classical diffusion equation employing Fourier's law.

Deviations between the predictions of the classical Fourier model and the dual-phase-lag model appear in applications involving a very fast heating rate and very thin layers; also, the deviation becomes significant in situations involving high frequency imposed thermal pulses.

Examples of a heating source having high frequencies are the laser and microwave heating sources. As an example, laser heating has become an active research area beginning with the employment of short pulse lasers in the fabrication of microstructures, laser patterning, laser processing of diamond films from carbon ion, implanted copper substrates, and laser surface heating.

On the other hand, multi-layer metal thin films are widely used in engineering applications since a single metal layer often cannot satisfy all mechanical, thermal, and electrical requirements. A better understanding of energy transfer in such multi-layer systems is critical in many applications. For example, high-power infrared-laser systems often use gold-coated metal mirrors because of their extremely high reflectivity, typically over 97%. Even with such high reflectivity, a small but significant portion of laser energy is still absorbed in the coating, which can cause excessive heating and thermal damage to the mirrors [6].

In the literature, numerous studies have been carried out to investigate the deviations between the predictions of the classical Fourier model and the dual-phase-lag model for different situations and under different operating conditions [7–17]. To the authors' best knowledge, the thermal behavior of a multi-layered thin slab carrying high-frequency periodic thermal signals under the effect of the dual-phase-lag heat conduction model

has not yet been investigated. The deviations between the predictions of the dual-phase-lag model and the classical Fourier law will be studied under different operating conditions and for two cases. Also, the effect of different thermal properties on the thermal behavior of the slab will be investigated. In the first case, the thermal harmonic behavior is a result of a fluctuating heating source; and in the second case, the thermal harmonic behavior is a result of a fluctuating imposed temperature at the boundary.

2. MATHEMATICAL FORMULATION

2.1. Case 1: Periodic Heating Source

Referring to Fig. 1, the following equations are applied for the two layers. It is assumed that there is a periodic heating source in the first layer and there is no volumetric heating source in the second layer. The subscripts 1 and 2 refer to the first and second layers, respectively.

$$\frac{1}{\alpha_1}\frac{\partial T_1}{\partial t}(t,r)+\frac{\bar{\tau}_{q1}}{\alpha_1}\frac{\partial^2 T_1}{\partial t^2}(t,r)=\nabla^2 T_1(t,r)+\bar{\tau}_{T1}\frac{\partial}{\partial t}\left[\nabla^2 T_1(t,r)\right]+\frac{1}{k_1}\left[g_1+\bar{\tau}_{q1}\frac{\partial g_1}{\partial t}(t,r)\right] \tag{8}$$

$$\frac{1}{\alpha_2}\frac{\partial T_2}{\partial t}(t,r)+\frac{\bar{\tau}_{q2}}{\alpha_2}\frac{\partial^2 T_2}{\partial t^2}(t,r)=\nabla^2 T_2(t,r)+\bar{\tau}_{T2}\frac{\partial}{\partial t}\left[\nabla^2 T_2(t,r)\right] \tag{9}$$

where

$$g_1=g_0\sin(\overline{w}t) \tag{10}$$

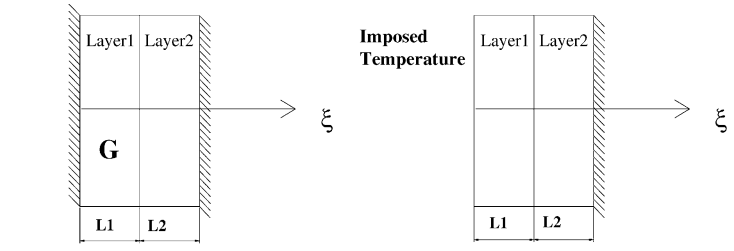

Case 1, pulsating heat source Case 2, pulsating imposed temperature

Fig. 1. Schematic diagram showing the problem geometry.

To generalize the results, the following non-dimensional variables are introduced:

$$\eta = \frac{\alpha_1 t}{L_1^2}, \quad \xi = \frac{x}{L_1}, \quad \tau_q = \frac{\alpha_1 \bar{\tau}_q}{L_1^2}, \quad \tau_T = \frac{\alpha_1 \bar{\tau}_T}{L_1^2},$$
$$\theta = \frac{T - T_\infty}{T_\infty}, \quad G_1 = \frac{g_1 L_1^2}{k_1 T_\infty}, \quad Q = \frac{q L_1}{k_1 T_\infty} \tag{11}$$

Hence, the governing equations in dimensionless form are given as

$$\frac{\partial \theta_1}{\partial \eta} + \tau_{q1} \frac{\partial^2 \theta_1}{\partial \eta^2} = \frac{\partial^2 \theta_1}{\partial \xi^2} + \tau_{T1} \frac{\partial^3 \theta_1}{\partial \eta \partial \xi^2} + G_1 + \tau_{q1} \frac{\partial G_1}{\partial \eta} \tag{12}$$

$$\frac{\partial \theta_2}{\partial \eta} + \tau_{q2} \frac{\partial^2 \theta_2}{\partial \eta^2} = \alpha_R \frac{\partial^2 \theta_2}{\partial \xi^2} + \alpha_R \tau_T^2 \frac{\partial^3 \theta_2}{\partial \eta \partial \xi^2} \tag{13}$$

where

$$\alpha_R = \frac{\alpha_2}{\alpha_1} \quad G_1 = G_0 \sin(w\eta) = G_0 \mathrm{Im}\{e^{iw\eta}\}$$
$$G_0 = \frac{g_0 L_1^2}{k_1 T_\infty} \quad w = \frac{\overline{w} L_1^2}{\alpha_1} \tag{14}$$

2.1.1. Boundary Conditions for Case 1

The two faces of the composite slab are insulated. At the interface between the two materials, we assume that there is no heat loss, i.e., the two materials are in perfect thermal contact. Therefore, their boundary conditions can be formulated as follows:
Boundary conditions:
At $x = 0$

$$\frac{\partial T_1}{\partial x}(t, 0) = 0 \tag{15}$$

At $x \; L_1 + L_2$

$$\frac{\partial T_2}{\partial x}(t, L_1 + L_2) = 0 \tag{16}$$

At $x \; L_1$ (at the contact point)

$$T_1(t, L_1) = T_2(t, L_1) \tag{17}$$
$$q_1(t, L_1) = q_2(t, L_1) \tag{18}$$

By applying the dimensionless variables in Eq. (11) to the boundary conditions, Eqs. (15)–(18), we get the following dimensionless boundary

conditions:
At $\xi = 0$

$$\frac{\partial \theta_1}{\partial \xi}(\eta, 0) = 0 \tag{19}$$

At $\xi = R$

$$\frac{\partial \theta_2}{\partial \xi}(\eta, R) = 0 \tag{20}$$

At $\xi = 1.0$ (at the contact point)

$$\theta_1(\eta, 1) = \theta_2(\eta, 1) \tag{21}$$

$$Q_1(\eta, 1) = Q_2(\eta, 1) \tag{22}$$

where $R = (L_1 + L_2)/L_1$.
Taking $L_1 = L_2$ and $R = 2$, Eqs. (12) and (13) assume the solution in the form:

$$\theta_1(\eta, \xi) = \mathrm{Im}\{W_1(\xi)\mathrm{e}^{iw\eta}\} \tag{23}$$

$$\theta_2(\eta, \xi) = \mathrm{Im}\{W_2(\xi)\mathrm{e}^{iw\eta}\} \tag{24}$$

where Im denotes "the imaginary part of" and i is the complex number $\sqrt{-1}$. As a result, Eqs. (12) and (13) are reduced to

$$\frac{\partial W_1}{\partial \xi^2} - \tau_1^2 W_1 = AA \tag{25}$$

$$\frac{\partial W_2}{\partial \xi^2} - \tau_2^2 W_2 = 0 \tag{26}$$

where the constants

$$\tau_1 = \sqrt{\frac{\mathrm{i}w - \tau_{q1} w^2}{1 + \mathrm{i}w\tau_{T1}}}$$

$$\tau_2 = \sqrt{\frac{\mathrm{i}w - \tau_{q2} w^2}{\alpha_R + \alpha_R i w \tau_{T2}}}$$

$$AA = \frac{-(G_0 + \mathrm{i}w\tau_{q1} G_0)}{(1 + \mathrm{i}w\tau_{T1})} \tag{27}$$

Equations (25) and (26) can be solved analytically as follows:

$$W_1 = C_1 \mathrm{e}^{\tau_1 \xi} + C_2 \mathrm{e}^{-\tau_1 \xi} - \frac{AA}{\tau_1^2} \tag{28}$$

$$W_2 = C_3 e^{\tau_2 \xi} + C_4 e^{-\tau_2 \xi} \tag{29}$$

The boundary conditions Eqs. (19)–(22) are transformed as follows: At $\xi = 0$

$$\frac{\partial W_1}{\partial \xi}(0) = 0 \tag{30}$$

At $\xi = R$

$$\frac{\partial W_2}{\partial \xi}(R) = 0 \tag{31}$$

At $\xi = 1$ (at the contact point)

$$W_1(1) = W_2(1) \tag{32}$$

$$\frac{\partial W_1}{\partial \xi}(1) = KR \frac{\partial W_2}{\partial \xi}(1) \tag{33}$$

where

$$KR = k_R \frac{(1 + iw\tau_{q1})}{(1 + iw\tau_{q2})} \frac{(1 + iw\tau_{T2})}{(1 + iw\tau_{T1})}$$

$$k_R = \frac{k_2}{k_1} \tag{34}$$

After applying the boundary conditions in Eqs. (30)–(33), the constants (C_1, C_2, C_3, and C_4) in Eqs. (28) and (29) can be determined:

$$C_1 = C_2 \tag{35}$$

$$C_3 = BBC_4 \tag{36}$$

$$C_2 = DDC_4 \tag{37}$$

$$C_4 = \frac{1}{(DDe^{\tau_1} + DDe^{-\tau_1} - BBe^{\tau_2} - e^{-\tau_2})} \frac{AA}{\tau_1^2} \tag{38}$$

where

$$BB = e^{-2\tau_2 R}$$

$$DD = KR \frac{(\tau_2 BBe^{\tau_2} - \tau_2 e^{-\tau_2})}{(\tau_1 e^{\tau_1} - \tau_1 e^{-\tau_1})} \tag{39}$$

Finally, the analytical solution for Eqs. (23) and (24) can be evaluated by using computer programs in "MATLAB".

2.2. Case 2: Periodic Imposed Temperature

Referring to Fig. 1, the following equations are applied for the two layers. It is assumed that there is no volumetric heating source in the two layers. The subscripts 1 and 2 refer to the first and second layers, respectively.

$$\frac{1}{\alpha_1}\frac{\partial T_1}{\partial t}(t,r)+\frac{\bar{\tau}_{q1}}{\alpha_1}\frac{\partial^2 T_1}{\partial t^2}(t,r)=\nabla^2 T_1(t,r)+\bar{\tau}_{T1}\frac{\partial}{\partial t}\left[\nabla^2 T_1(t,r)\right] \quad (40)$$

$$\frac{1}{\alpha_2}\frac{\partial T_2}{\partial t}(t,r)+\frac{\bar{\tau}_{q2}}{\alpha_2}\frac{\partial^2 T_2}{\partial t^2}(t,r)=\nabla^2 T_2(t,r)+\bar{\tau}_{T2}\frac{\partial}{\partial t}\left[\nabla^2 T_2(t,r)\right] \quad (41)$$

To generalize the results, the following non-dimensional variables are introduced:

$$\eta=\frac{\alpha_1 t}{L_1^2},\quad \xi=\frac{x'}{L_1},\quad \tau_q=\frac{\alpha_1\bar{\tau}_q}{L_1^2},\quad \tau_T=\frac{\alpha_1\bar{\tau}_T}{L_1^2},\quad \theta=\frac{T}{T_\infty},\quad Q=\frac{qL_1}{k_1T_\infty} \quad (42)$$

Hence, the governing equations in dimensionless form are given as

$$\frac{\partial\theta_1}{\partial\eta}+\tau_{q1}\frac{\partial^2\theta_1}{\partial\eta^2}=\frac{\partial^2\theta_1}{\partial\xi^2}+\tau_{T1}\frac{\partial^3\theta_1}{\partial\eta\partial\xi^2} \quad (43)$$

$$\frac{\partial\theta_2}{\partial\eta}+\tau_{q2}\frac{\partial^2\theta_2}{\partial\eta^2}=\alpha_R\frac{\partial^2\theta_2}{\partial\xi^2}+\alpha_R\tau_{T2}\frac{\partial^3\theta_2}{\partial\eta\partial\xi^2} \quad (44)$$

where

$$\alpha_R=\frac{\alpha_2}{\alpha_1}$$

2.2.1. Boundary Conditions for Case 2

One face of the composite slab is insulated while the other face was imposed with a fluctuating temperature. At the interface between the two materials, we assume that there is no heat loss, i.e., the two materials are in perfect thermal contact.

Therefore, their boundary conditions can be summarized as follows:
Boundary conditions:
At $x=0$

$$T_1(t,0)=T_0\sin(\overline{w}t) \quad (45)$$

At $x=L_1+L_2$

$$\frac{\partial T_2}{\partial x}(t,L_1+L_2)=0 \quad (46)$$

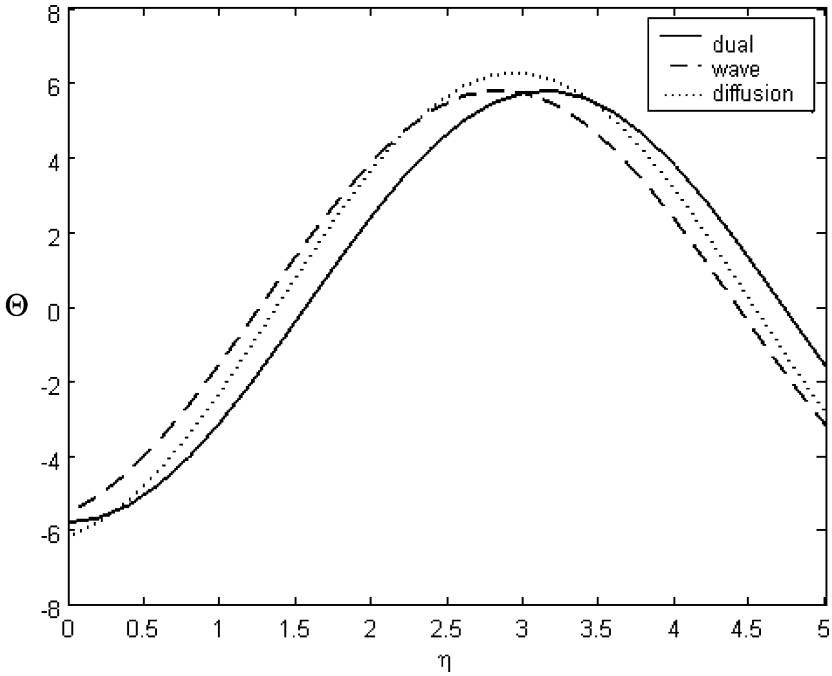

Fig. 2. Effect of angular frequency on the transient temperature distribution at $\xi = 0.5$ under the effect of a periodic heating source; $\tau_{q1} = 0.4348$ $\tau_{q2} = 0.7438$, $\tau_{T1} = 70.833$, $\tau_{T2} = 89.286$, $\alpha_R = 1.47$, $k_R = 1.085$, $\omega = 1.0$, $G_0 = 10.0$.

At $x = L_1$ (at the contact point)

$$T_1(t, L_1) = T_2(t, L_1) \tag{47}$$

$$q_1(t, L_1) = q_2(t, L_1) \tag{48}$$

By applying the dimensionless variables, Eq. (42), to the boundary conditions, Eqs. (45)–(48), we get the following dimensionless boundary conditions:
At $\xi = 0$

$$\theta_1(\eta, 0) = \theta_0 \sin(w\eta) = \theta_0\{\mathrm{Im}e^{iw\eta}\} \tag{49}$$

At $\xi = R$

$$\frac{\partial \theta_2}{\partial \xi}(\eta, R) = 0 \tag{50}$$

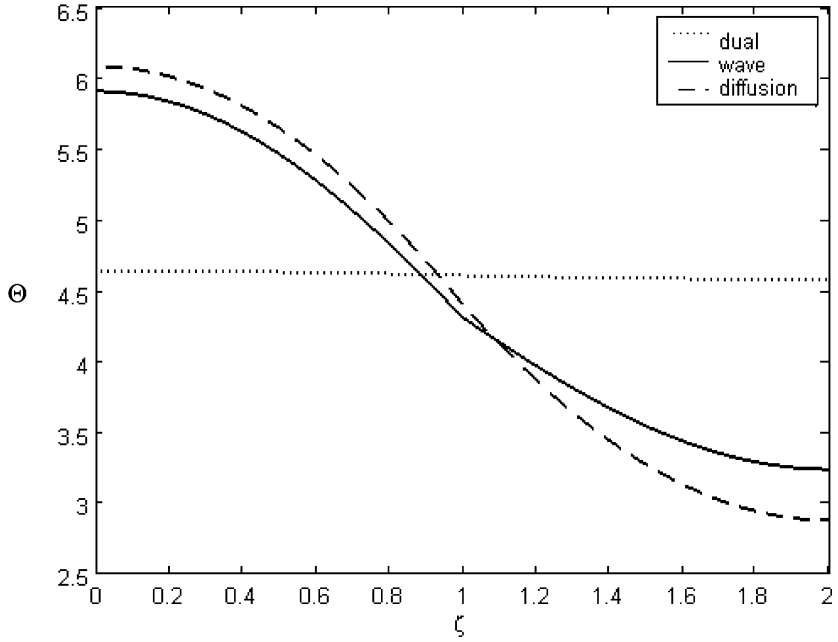

Fig. 3. Effect of angular frequency on the spatial temperature distribution at $\eta = 1.5$ under the effect of a periodic heating source; $\tau_{q1} = 0.4348$, $\tau_{q2} = 0.7438$, $\tau_{T1} = 70.833$, $\tau_{T2} = 89.286$, $\alpha_R = 1.47$, $k_R = 1.085$, $\omega = 1.0$, $G_0 = 10.0$.

At $\xi = 1$ (at the contact point)

$$\theta_1(\eta, 1) = \theta_2(\eta, 1) \tag{51}$$

$$Q_1(\eta, 1) = Q_2(\eta, 1) \tag{52}$$

where

$$R = \frac{L_1 + L_2}{L_1}, \quad \theta_0 = \frac{T_0}{T_\infty}, \quad w = \frac{\overline{w} L_1^2}{\alpha_1} \tag{53}$$

Taking $L_1 = L_2$ and $R = 2$,

Equations (43) and (44) assume a solution in the form,

$$\theta_1(\eta, \xi) = \mathrm{Im}\{W_1(\xi) \mathrm{e}^{\mathrm{i}w\eta}\} \tag{54}$$

$$\theta_2(\eta, \xi) = \mathrm{Im}\{W_2(\xi) \mathrm{e}^{\mathrm{i}w\eta}\} \tag{55}$$

As a result, Eqs. (43) and (44) are reduced to

$$\frac{\partial W_1}{\partial \xi^2} - \tau_1^2 W_1 = 0 \tag{56}$$

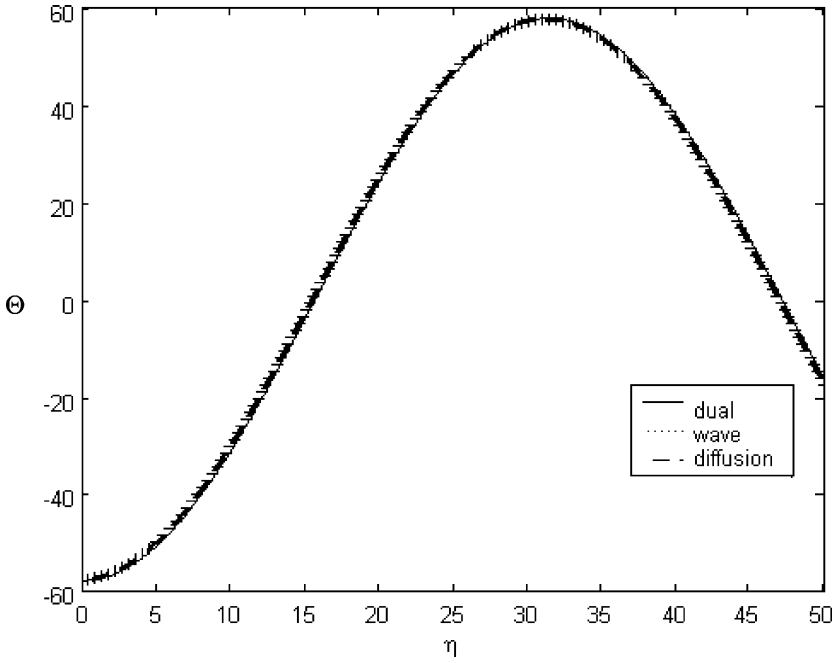

Fig. 4. Effect of angular frequency on the transient temperature distribution at $\xi = 0.5$ under the effect of a periodic heating source; $\tau_{q1} = 0.4348$, $\tau_{q2} = 0.7438$, $\tau_{T1} = 70.833$, $\tau_{T2} = 89.286$, $\alpha_R = 1.47$, $k_R = 1.085$, $\omega = 0.1$, $G_0 = 10.0$.

$$\frac{\partial W_2}{\partial \xi^2} - \tau_2^2 W_2 = 0 \tag{57}$$

where the constants are as defined in Eq. (27)

Equations (56) and (57) can be solved analytically as follows:

$$W_1 = C_1 e^{\tau_1 \xi} + C_2 e^{-\tau_1 \xi} \tag{58}$$

$$W_2 = C_3 e^{\tau_2 \xi} + C_4 e^{-\tau_2 \xi} \tag{59}$$

The boundary conditions, Eqs. (49)–(52), are transformed as follows:
At $\xi = 0$

$$W_1(0) = 0 \tag{60}$$

At $\xi = R$

$$\frac{\partial W_2}{\partial \xi}(R) = 0 \tag{61}$$

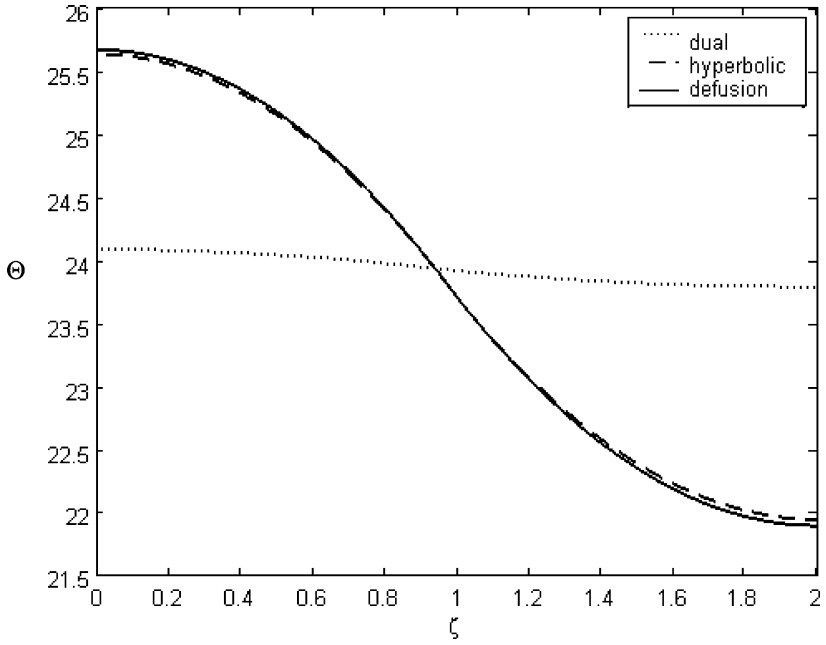

Fig. 5. Effect of angular frequency on the spatial temperature distribution at $\eta = 20.0$ under the effect of a periodic heating source; $\tau_{q1} = 0.4348$, $\tau_{q2} = 0.7438$, $\tau_{T1} = 70.833$, $\tau_{T2} = 89.286$, $\alpha_R = 1.47$, $k_R = 1.085$, $\omega = 0.1$, $G_0 = 10.0$.

At $\xi = 1$ (at the contact point)

$$W_1(1) = W_2(1) \tag{62}$$

$$\frac{\partial W_1}{\partial \xi}(1) = KR \frac{\partial W_2}{\partial \xi}(1) \tag{63}$$

where KR is as defined in Eq. (34).

After applying the boundary conditions in Eqs. (60)–(63), the constants (C_1, C_2, C_3, and C_4) in Eqs. (58) and (59) can be determined:

$$C_1 = \theta_0 - C_2 \tag{64}$$

$$C_3 = BBC_4 \tag{65}$$

$$C_2 = DDC_4 + EE \tag{66}$$

$$C_4 = \frac{(\theta_0 - EE)e^{\tau_1} + EEe^{-\tau_1}}{(BBe^{\tau_2} + e^{-\tau_2} + DDe^{\tau_1} - DDe^{-\tau_1})} \tag{67}$$

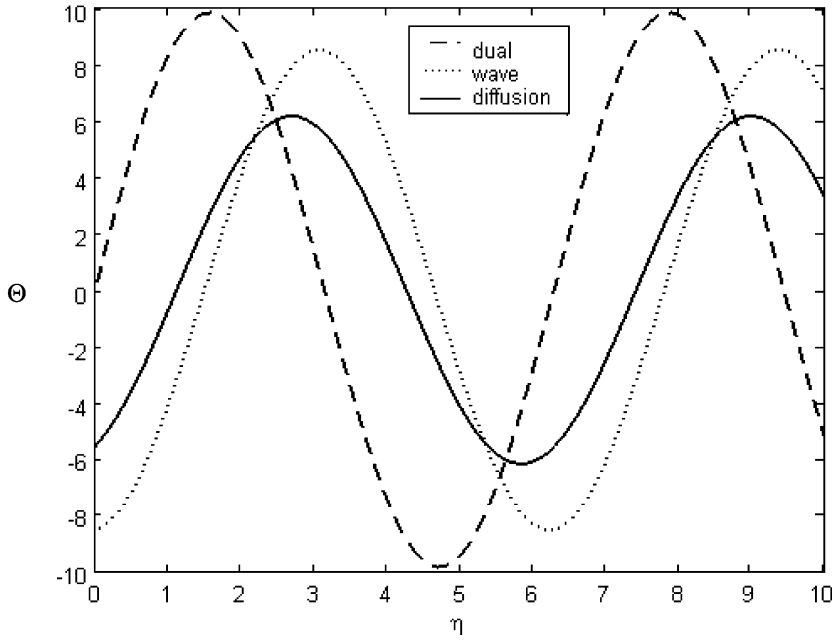

Fig. 6. Effect of angular frequency on the transient temperature distribution at $\xi = 1.5$ under the effect of a periodic imposed temperature; $\tau_{q1} = 0.4348$, $\tau_{q2} = 0.7438$, $\tau_{T1} = 70.833$, $\tau_{T2} = 89.286$, $\alpha_R = 1.47$, $k_R = 1.085$, $\omega = 1.0$, $\theta_0 = 10.0$.

where

$$BB = e^{-2\tau_2 R}, \quad DD = KR\frac{(\tau_2 e^{-\tau_2} - \tau_2 BB e^{\tau_2})}{(\tau_1 e^{\tau_1} + \tau_1 e^{-\tau_1})}, \quad EE = \frac{\tau_1 \theta_0 e^{\tau_1}}{(\tau_1 e^{\tau_1} + \tau_1 e^{-\tau_1})} \tag{68}$$

Finally, the analytical solution for Eqs. (54) and (55) can be evaluated by using computer programs in "MATLAB."

3. RESULTS AND DISCUSSION

Figures 2–7 show the effect of the angular frequency ω on the transient and spatial temperature distribution of the slab under the effect of the periodic heating source and periodic imposed temperature. It is clear from these figures that the deviations among the predictions of the three models increase as ω increases. An increase in ω will increase the effect of the time delay between the heat flux and the temperature gradient, and the deviations among the three models will increase. This implies that the classical diffusion model gives accurate predictions for the plate thermal

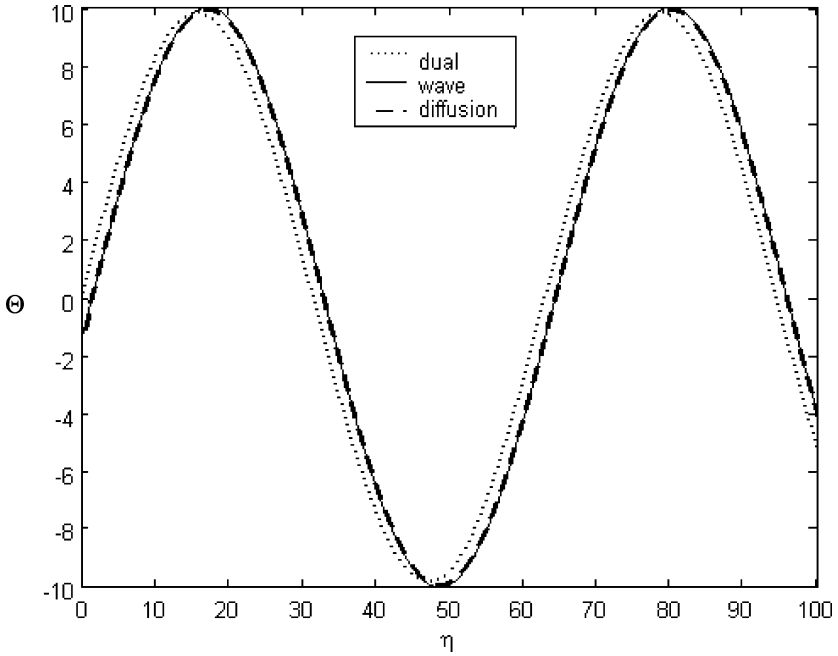

Fig. 7. Effect of angular frequency on the transient temperature distribution at $\xi = 1.5$ under the effect of a periodic imposed temperature; $\tau_{q1} = 0.4348$, $\tau_{q2} = 0.7438$, $\tau_{T1} = 70.833$, $\tau_{T2} = 89.286$, $\alpha_R = 1.47$, $k_R = 1.085$, $\omega = 0.1$, $\theta_0 = 10.0$.

behavior when ω is very small. On the other hand, the use of the dual-phase-lag model or wave model becomes a necessity when ω increases. In addition, it is clear from these figures that the deviations between the predictions of the wave model and the diffusion model are smaller than the deviations between the dual-phase-lag model and the diffusion model. Also, it is noticed that the deviations among the predictions of the three models become significant when $\omega > 1.0$. This corresponds to $\varpi > \frac{\alpha_1}{L_1^2}$. Most metal films have α of order 10^{-4} $m^2 \cdot s^{-1}$ and $L_1 = 10^{-8}$. This implies that the use of the dual-phase-lag model becomes a necessity when the frequency of the heating source is larger than $10^{12}\,s^{-1}$. Figures 2, 6, 8, and 9 show the temperature distribution for the three models for different values of dimensionless phase lag in temperature gradient and heat flux. The figures show that the deviations among the predictions of the three models increase as the dimensionless phase lag in the temperature gradient and heat flux increases. And it is significant for $\tau_{q1} > 2.718 \times 10^{-4}$. This corresponds to $L_1^2 < \frac{\overline{\tau_{q1}} \times \alpha_1}{2.718 \times 10^{-4}}$. For most metals,

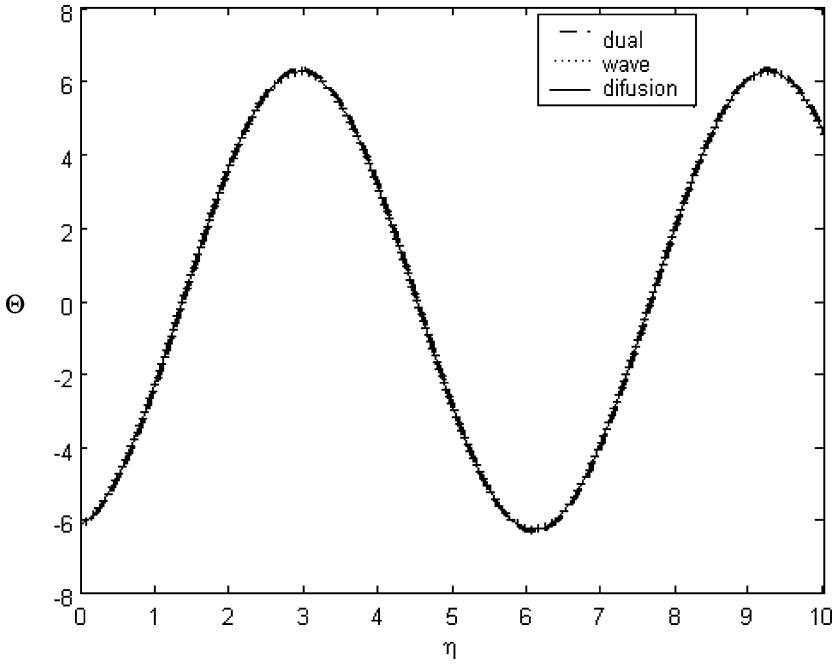

Fig. 8. Deviations in temperature distribution between the three models at $\xi = 0.5$ under the effect of a periodic heating source; $\tau_{q1} = 2.718 \times 10^{-4}$, $\tau_{q2} = 4.649 \times 10^{-4}$, $\tau_{T1} = 0.0443$, $\tau_{\{T_2\}} = 0.0558$, $\alpha_R = 1.47$, $k_R = 1.085$, $\omega = 1.0$, $G_0 = 10.0$.

α is of order 10^{-4} $m^2 \cdot s^{-1}$, $\overline{\tau}_q$ is of order 10^{-12} s, and $\overline{\tau}_T$ is of order 10^{-10} s. As a result, the use of the dual-phase-lag model is necessary when the metal film thickness is of order 10^{-6} m.

4. CONCLUSION

The thermal behavior of a two-layered thin slab under the effect of periodic heating signals is investigated using three different heat conduction models: diffusion, wave, and dual-phase-lag heat conduction models. The periodic thermal behavior is a result of a periodic heating source or a periodic imposed temperature at the boundary. It is found that the deviations among the three models increase as the frequency of the signals increases and as the dimensionless thickness of the slab decreases. Also, it is found that the deviations increase as the dimensionless phase lag in temperature gradient and heat flux increase. It is found that the use of the dual-phase-lag model is necessary when the metal film thickness

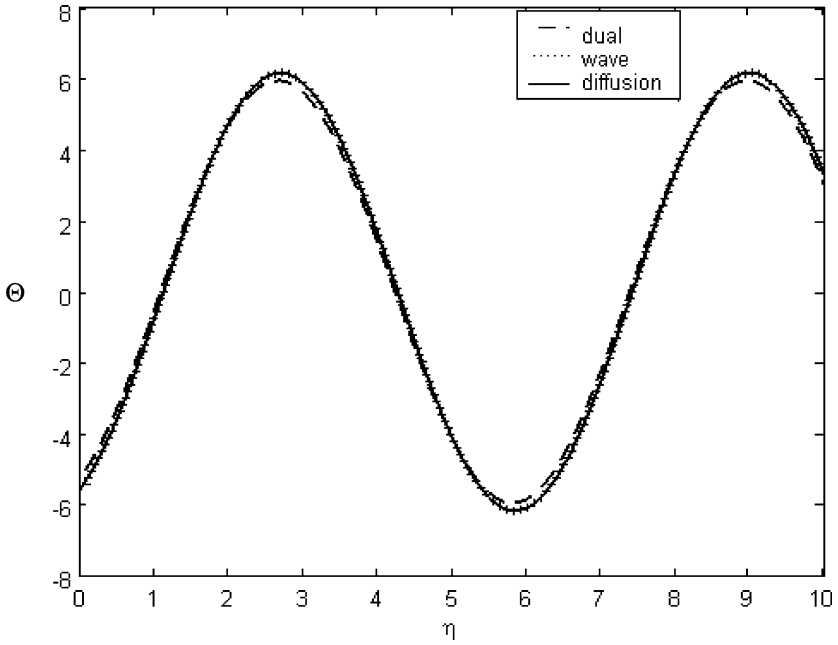

Fig. 9. Deviations in temperature distribution between the three models at $\xi = 1.5$ under the effect of a periodic imposed temperature; $\tau_{q1} = 2.718 \times 10^{-4}$, $\tau_{q2} = 4.649 \times 10^{-4}$, $\tau_{T1} = 0.0443$, $\tau_{T2} = 0.0558$, $\alpha_R = 1.47$, $k_R = 1.085$, $\omega = 1.0$, $\theta_0 = 10.0$.

is of order 10^{-6} m and the angular frequency of the signals is of order 10^{12} rad $\cdot$ s^{-1}. It is found that the temperature distribution within the slab increases as the thermal conductivity ratio (k_2/k_1) decreases and the thermal diffusivity ratio (α_2/α_1) increases. Analytical closed-form solutions are obtained for the temperature distribution within the slab.

NOMENCLATURE

c Specific heat capacity (J $\cdot$ kg^{-1} $\cdot$ K^{-1})
g Heating source per unit volume (W $\cdot$ m^{-3})
g_0 Amplitude of the heating source (W $\cdot$ m^{-3})
G Dimensionless heating source, $\frac{gL_1^2}{k_1 T_\infty}$
G_0 Amplitude of the dimensionless heating source, $\frac{g_0 L_1^2}{k_1 T_\infty}$
L_1 Thickness of the first plate, m

L_2 Thickness of the second plate, m
k Thermal conductivity ($W \cdot m^{-1} \cdot K^{-1}$)
k_R Thermal conductivity ratio k_2/k_1
q Conduction heat flux, ($W \cdot m^{-2}$)
t Time, s
T Temperature, K
T_0 Amplitude of the periodic imposed temperature, K
T_∞ Ambient temperature, K
x x direction
r Spatial distance

Greek Symbols

α Thermal diffusivity ($m^2 \cdot s^{-1}$)
α_R Thermal diffusivity ratio α_2/α_1
η Dimensionless time, $\frac{t\alpha_1}{L_1^2}$
ρ Density ($kg \cdot m^{-3}$)
θ_1 Dimensionless temperature for case 1, $\frac{T-T_\infty}{T_\infty}$
θ_2 Dimensionless temperature for case 2, $\frac{T}{T_\infty}$
θ_0 Dimensionless amplitude of the imposed temperature, $\frac{T_0}{T_\infty}$
τ_T Dimensionless phase-lag in the temperature gradient, $\frac{\overline{\tau_T}\alpha_1}{L_1^2}$
τ_q Dimensionless phase-lag in the heat flux, $\frac{\overline{\tau_q}\alpha_1}{L_1^2}$
$\bar{\tau}_q$ Phase-lag in the heat flux vector, s
$\bar{\tau}_T$ Phase-lag in the temperature gradient, s
w Dimensionless periodic source frequency, $\frac{\tilde{\omega}L_1^2}{\alpha_1}$
$\overline{w}$ Periodic source frequency, Hz
ξ Dimensionless transverse coordinate, $\frac{x}{L_1}$

Subscripts

∞ Ambient conditions
1 First layer
2 Second layer

REFERENCES

1. C. Cattaneo, *Comptes Rendus* **247**:431 (1958).
2. P. Vernotte, *Comptes Rendus* **252**:2190 (1961).
3. D. Y. Tzou, *ASME J. Heat Transfer* **117**:8 (1995).
4. D. Y. Tzou, *Int. J. Heat Mass Transfer.* **38**:3231 (1995).
5. D. Y. Tzou, *AIAA J. Thermophys. Heat Transfer* **9**:686 (1995).

6. P. M. Morse and H. Feshbach, *Methods of Theoretical Physics,* Vo1.1 (McGraw-Hill, New York, 1953).
7. M. A. Al-Nimr and V. S. Arpaci, *J. Appl. Phys.* **85**:no. 5 (1999).
8. M. A. Al-Nimr and V. S. Arpaci, *Int. J. Heat Mass Transfer* **43**:2021 (2000).
9. N. S. Al-Huniti and M. A. Al-Nimr, *J. Thermal Stresses* **23**:293 (2000).
10. M. A. Al-Nimr and M. Naji, *Int. J. Thermophys.* **21**:281 (2000).
11. M. A. Al-Nimr, O. M. Haddad, and V. Arpaci, *Heat Mass Transfer* **35**:459 (1999).
12. M. A. Al-Nimr and M. Naji, *Heat Mass Transfer* **35**:493 (1999).
13. M. A. Al-Nimr and N. S. Al-Huniti, *J. Thermal Stresses* **23**:731 (2000).
14. S. Kiwan and M. A. Al-Nimr, *Jpn. J. Appl. Phys.* **39**:4245 (2000).
15. M. Naji, M. A. Al-Nimr, and N. S. Al-Huniti, *J. Thermal Stresses* **24**:399 (2001).
16. M. A. Al-Nimr and M. A. Hader, *Heat Transfer Eng. J.* **22**:1 (2001).
17. M. A. Al-Nimr and S. Kiwan, *Int. J. Heat Mass Transfer* **44**:1013 (2001).